

Characterization of peptide binding to the SARS-CoV-2 host factor neuropilin

Amie Jobe¹ and Ranjit Vijayan^{1,2,*}

¹ Department of Biology, College of Science, United Arab Emirates University, PO Box 15551, Al Ain, United Arab Emirates.

² The Big Data Analytics Center, United Arab Emirates University, PO Box 15551, Al Ain, United Arab Emirates.

* Correspondence: ranjit.v@uaeu.ac.ae

SUPPLEMENTARY INFORMATION

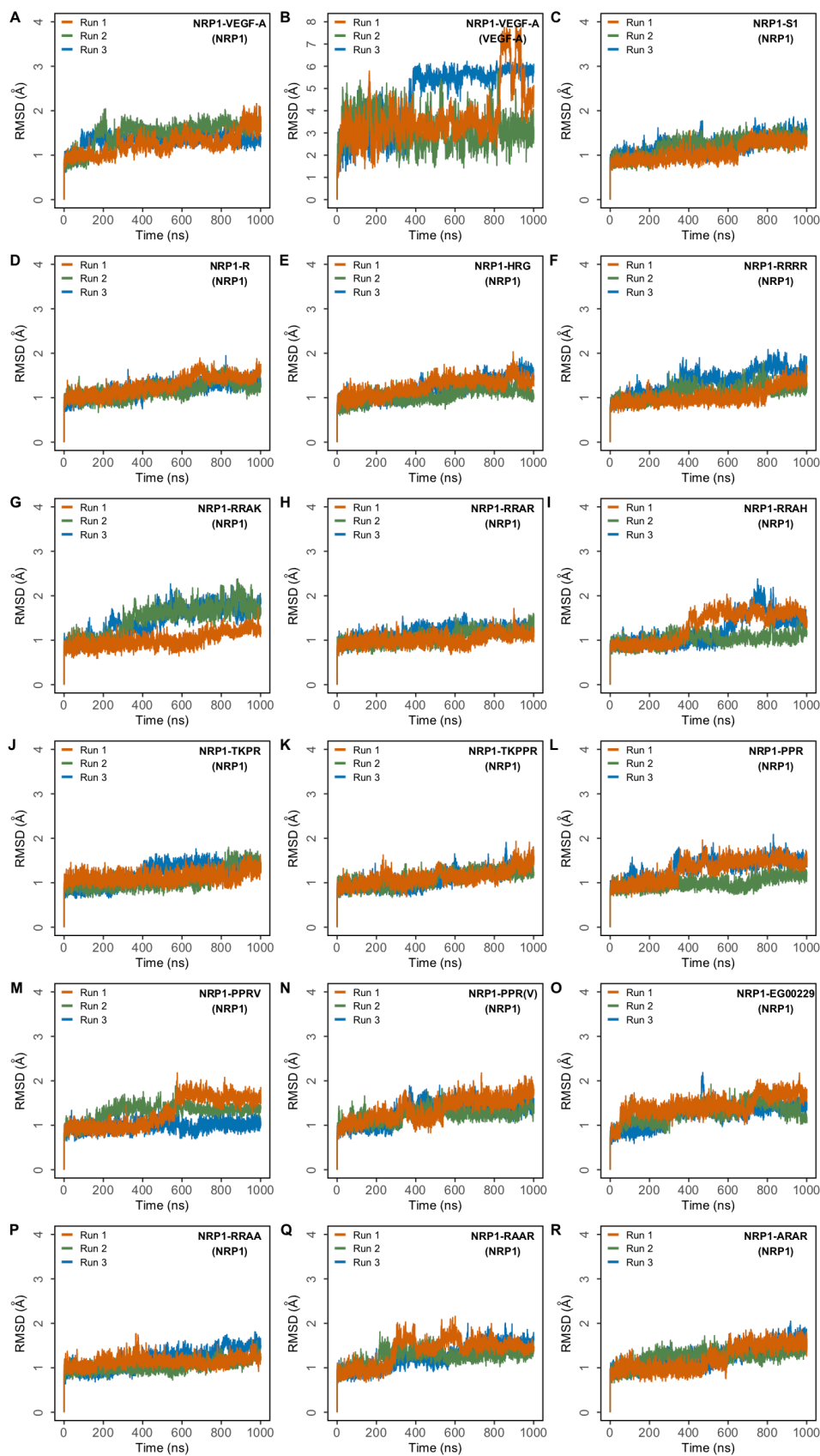


Figure S1. Root mean square deviation (RMSD) of protein C α atoms with respect to the initial structure obtained from three independent runs of the different peptides bound to NRP1. (A) NRP1 in the NRP1–VEGF-A complex; (B) VEGF-A in the NRP1–VEGF-A complex; (C) NRP1 in the NRP1–S1 complex; (D) NRP1 in the NRP1–R complex; (E) NRP1 in the NRP1–HRG complex; (F) NRP1 in the NRP1–RRRR complex; (G) NRP1 in the NRP1–RRAK complex; (H) NRP1 in the NRP1–RRAR complex; (I) NRP1 in the NRP1–RRAH complex; (J) NRP1 in the NRP1–TKPR complex; (K) NRP1 in the NRP1–TKPPR complex; (L) NRP1 in the NRP1–PPR complex; (M) NRP1 in the NRP1–PPRV complex; (N) NRP1 in the NRP1–PPR(V) complex; (O) NRP1 in the NRP1–EG00229 complex; (P) NRP1 in the NRP1–RRAA complex; (Q) NRP1 in the NRP1–RAAR complex; (R) NRP1 in the NRP1–ARAR complex.

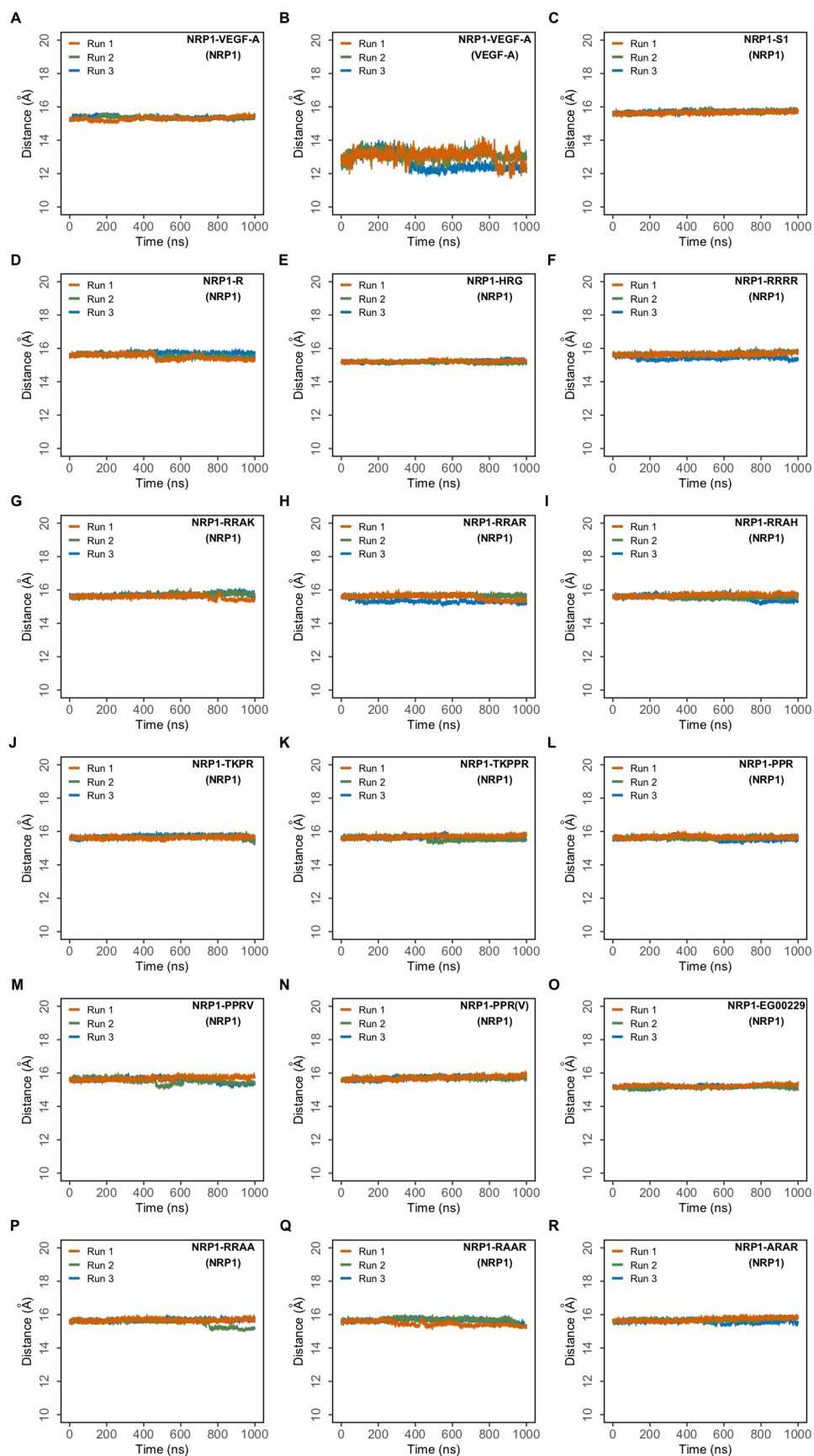


Figure S2. Radius of gyration (R_g) of NRP1 or bound protein. Three $1 \mu\text{s}$ simulations of each NRP1-peptide complex were performed. **(A)** R_g of NRP1 in NRP1-VEGF-A complex; **(B)** R_g of VEGF-A in NRP1-VEGF-A complex; **(C)** R_g of NRP1 in NRP1-S1 complex; **(D)** R_g of NRP1 in NRP1-R complex; **(E)** R_g of NRP1 in NRP1-HRG complex; **(F)** R_g of NRP1 in NRP1-RRRR complex; **(G)** R_g of NRP1 in NRP1-RAAK complex; **(H)** R_g of NRP1 in NRP1-RRAR complex; **(I)** R_g of NRP1 in NRP1-RAAH complex; **(J)** R_g of NRP1 in NRP1-TKPR complex; **(K)** R_g of NRP1 in NRP1-TKPPR complex; **(L)** R_g of NRP1 in NRP1-PPR complex; **(M)** R_g of NRP1 in NRP1-PPRV complex; **(N)** R_g of NRP1 in NRP1-PPR(V) complex; **(O)** R_g of NRP1 in the NRP1-EG00229 complex; **(P)** R_g of NRP1 in the NRP1-RAAA complex; **(Q)** R_g of NRP1 in the NRP1-RAAR complex; **(R)** R_g of NRP1 in the NRP1-ARAR complex.

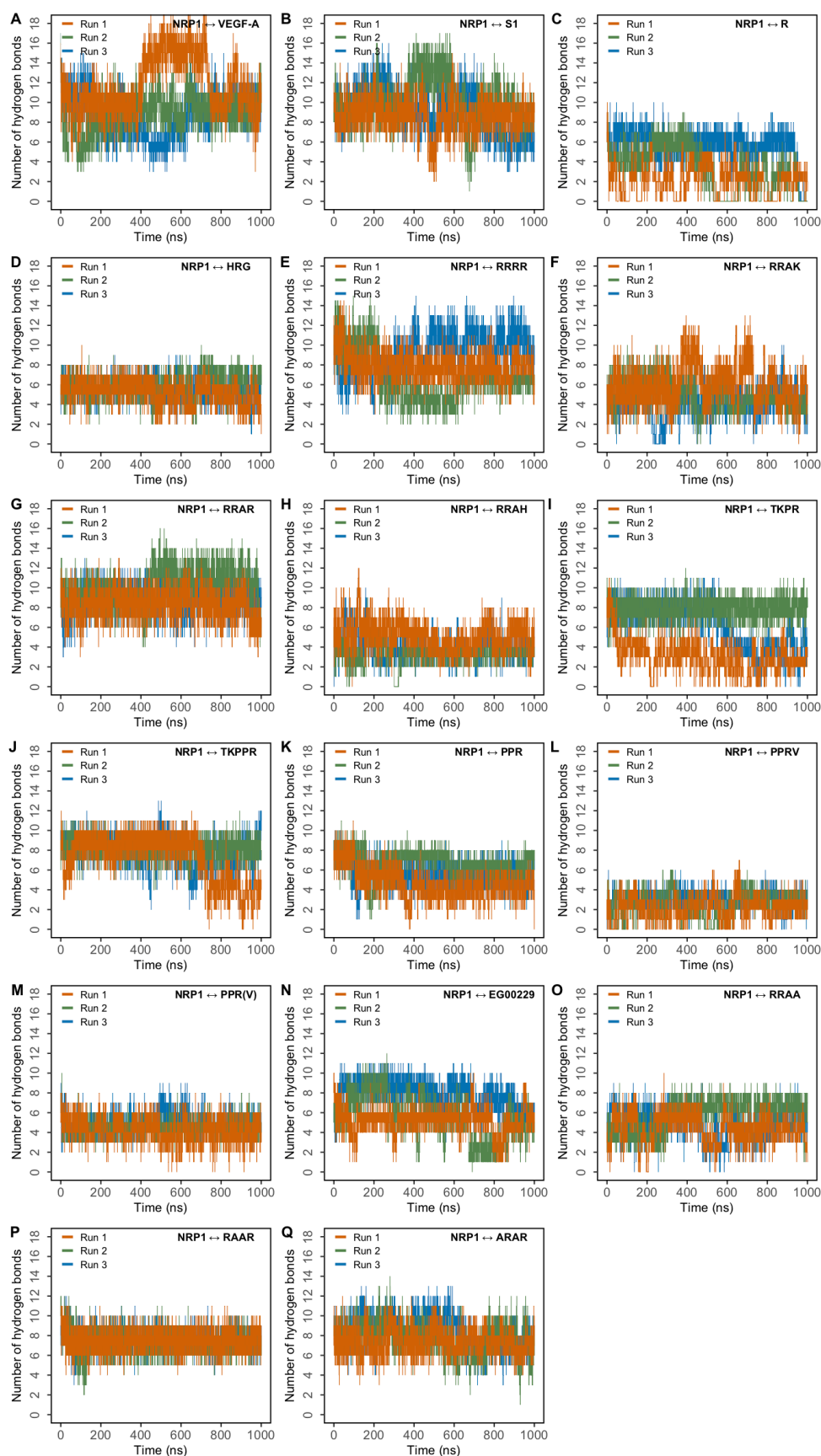


Figure S3. Number of intermolecular hydrogen bonds formed between NRP1 and the bound peptide from three independent 1 μ s simulations. (A) Between NRP1 and VEGF-A; (B) between NRP1 and S1; (C) between NRP1 and R; (D) between NRP1 and HRG; (E) between NRP1 and RRRR; (F) between NRP1 and RRAK; (G) between NRP1 and RRAR; (H) between NRP1 and RRAH; (I) between NRP1 and TKPR; (J) between NRP1 and TKPPR; (K) between NRP1 and PPR; (L) between NRP1 and PPRV; (M) between NRP1 and PPR(V); (N) between NRP1 and EG00229; (O) between NRP1 and RRAA; (P) between NRP1 and RAAR; (Q) between NRP1 and ARAR.

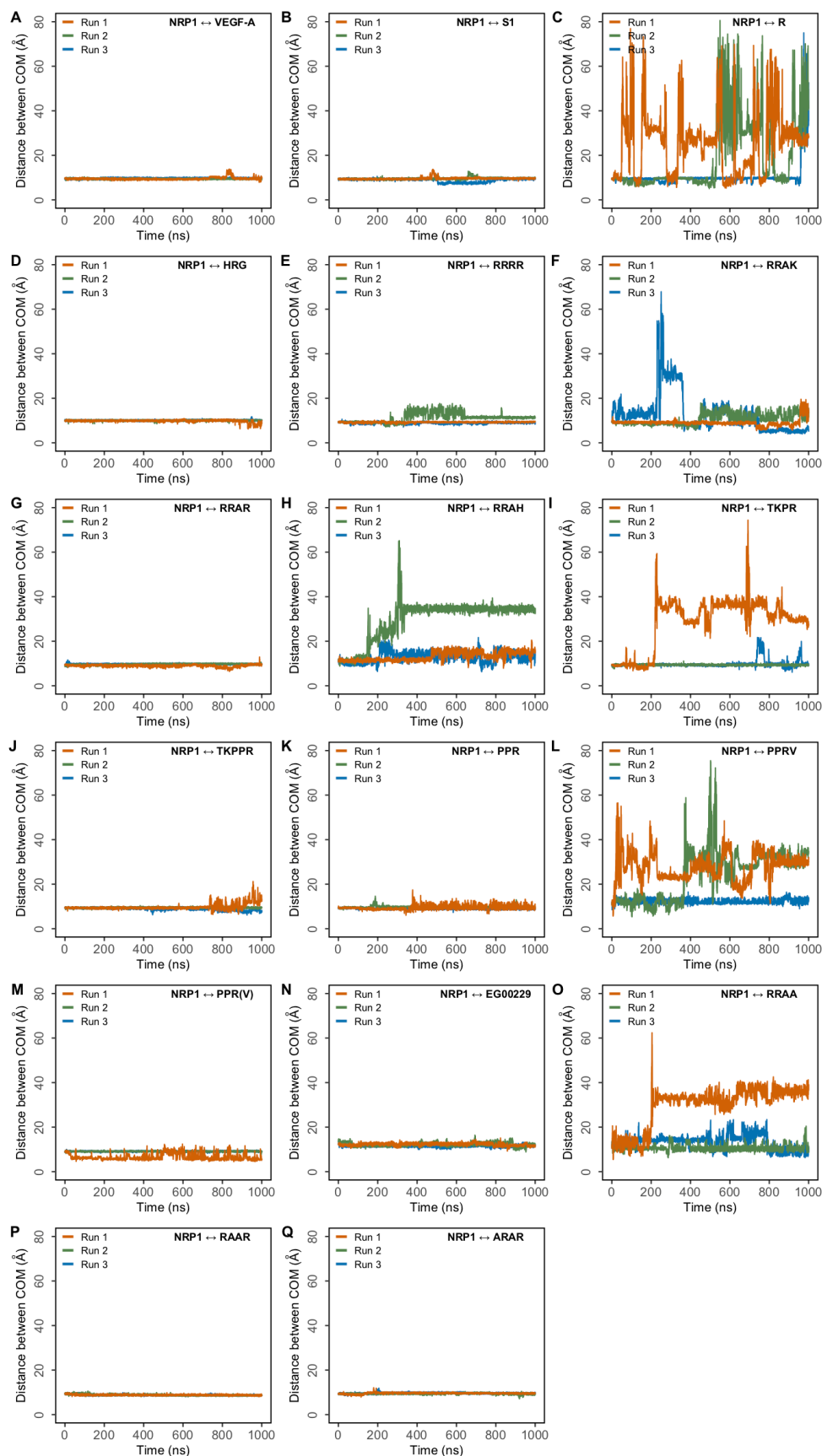


Figure S4: Distance between the center of mass (COM) of $C\alpha$ atom of NRP1:Asp320 and $C\alpha$ atom of the peptide residue equivalent to the terminal arginine (position 685). (A) between NRP1 and VEGF-A; (B) between NRP1 and S1; (C) between NRP1 and R; (D) between NRP1 and HRG; (E) between NRP1 and RRRR; (F) between NRP1 and RRAK; (G) between NRP1 and RRAR; (H) between NRP1 and RRAH; (I) between NRP1 and TKPR; (J) between NRP1 and TKPPR; (K) between NRP1 and PPR; (L) between NRP1 and PPRV; (M) between NRP1 and PPR(V); (N) between NRP1 and EG00229; (O) between NRP1 and RRAA; (P) between NRP1 and RAAR; (Q) between NRP1 and ARAR.

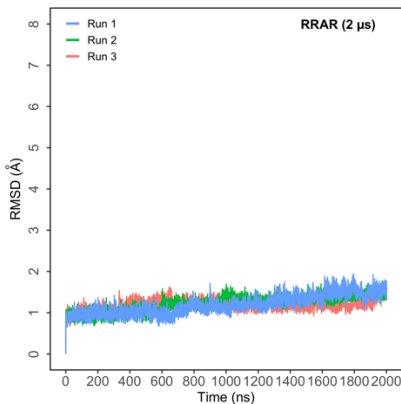


Figure S5: Root mean square deviation (RMSD) of protein $C\alpha$ atoms with respect to the initial structure obtained from three independent 2 μ s runs of the peptide RRAR bound to NRP1.

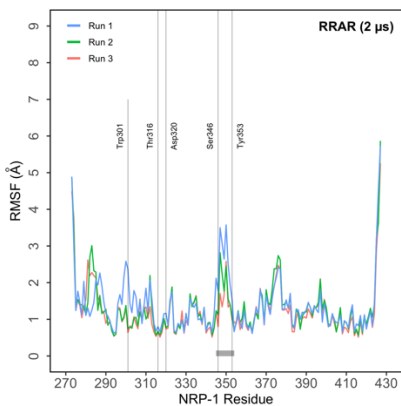


Figure S6: Root mean square fluctuation (RMSF) of protein $C\alpha$ atoms obtained from three independent 2 μ s runs of the peptide RRAR bound to NRP.

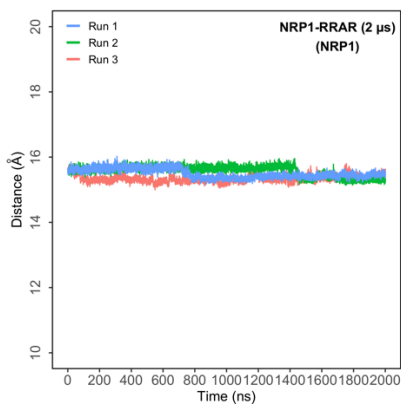


Figure S7. Radius of gyration (R_g) of NRP1 from three independent 2 μ s simulations of RRAR bound to NRP1.

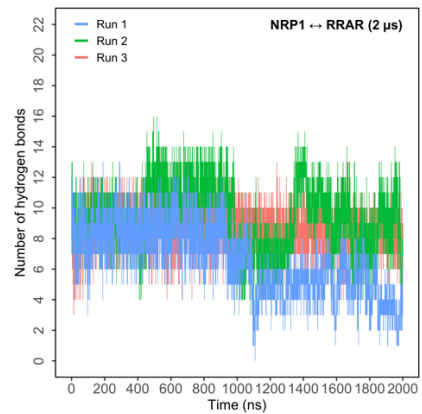


Figure S8. Number of intermolecular hydrogen bonds formed between NRP1 and the bound RRAR peptide from three independent 2 μ s simulations.

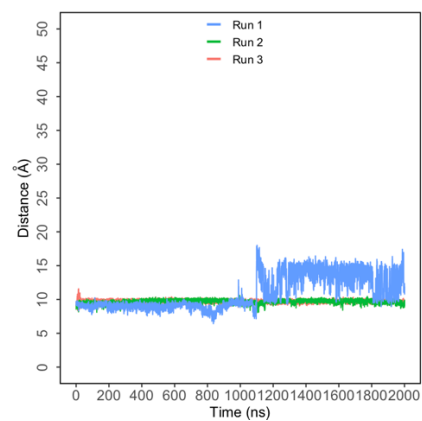


Figure S9: Distance between the center of mass of C α atom of NRP1:Asp320 and C α atom of C-terminal arginine of RRAR from three independent 2 μ s simulations.

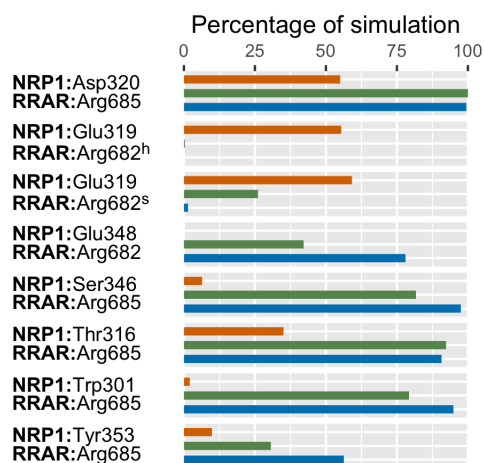


Figure S10: The percentage of simulation time during which intermolecular polar contacts were retained between NRP1 and the peptide RRAR in three independent 2 μ s runs.

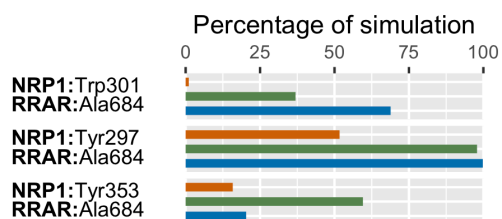


Figure S11: The percentage of simulation time during which intermolecular hydrophobic contacts were retained between NRP1 and the peptide RRAR in three independent 2 μ s runs.

Table S1. Free energy of binding (ΔG_{bind}) of peptides in the simulated systems computed using the MM-GBSA method. Rows in red text represent simulations in which the peptide dissociates from NRP1.

Peptide	Run	ΔG_{bind} (kcal/mol)		Peptide	Run	ΔG_{bind} (kcal/mol)
VEGF A	run1	-85.81 \pm 18.66		RRRR	run1	-79.22 \pm 6.48
	run2	-67.34 \pm 11.27			run2	-53.71 \pm 17.68
	run3	-82.07 \pm 18.59			run3	-80.54 \pm 12.06
HRG	run1	-54.44 \pm 5.63		RRAH	run1	-58.28 \pm 12.83
	run2	-57.00 \pm 4.91			run2	-43.40 \pm 22.11
	run3	-57.53 \pm 4.29			run3	-41.66 \pm 12.47
S1	run1	-73.14 \pm 11.75		RRAK	run1	-58.86 \pm 11.55
	run2	-90.93 \pm 16.09			run2	-48.88 \pm 10.65
	run3	-86.31 \pm 14.15			run3	-47.68 \pm 19.12
R	run1	-15.68 \pm 10.18		TKPPR	run1	-57.68 \pm 14.23
	run2	-26.31 \pm 17.57			run2	-63.05 \pm 5.14
	run3	-43.65 \pm 10.86			run3	-74.50 \pm 12.19
PPR	run1	-44.62 \pm 10.76		TKPR	run1	-23.67 \pm 11.80
	run2	-61.39 \pm 6.14			run2	-67.33 \pm 5.31
	run3	-56.56 \pm 5.11			run3	-51.48 \pm 19.13
PPRV	run1	-36.60 \pm 10.45		ARAR	run1	-72.63 \pm 7.79
	run2	-37.90 \pm 13.62			run2	-66.50 \pm 7.86
	run3	-40.26 \pm 4.85			run3	-74.16 \pm 6.97
PPR(V)	run1	-57.49 \pm 7.16		RRAA	run1	-45.00 \pm 9.49
	run2	-64.12 \pm 5.11			run2	-54.63 \pm 6.46
	run3	-68.26 \pm 6.97			run3	-50.23 \pm 10.64
RRAR	run1	-72.97 \pm 7.26		RAAR	run1	-70.05 \pm 5.27
	run2	-84.60 \pm 10.84			run2	-68.95 \pm 4.78
	run3	-80.68 \pm 7.38			run3	-71.53 \pm 6.08
RRAR (2 μ s)	run1	-59.37 \pm 15.56		EG00229	run1	-78.92 \pm 5.70
	run2	-82.30 \pm 10.52			run2	-76.74 \pm 10.52
	run3	-80.81 \pm 7.67			run3	-93.05 \pm 7.67